ROYAL SOCIETY OF CHEMISTRY

PAPER

Check for updates

Citric acid crosslinking of arabinoxylan engenders a stimuli-responsive hydrogel as a smart material for intelligent drug delivery

Syed Nasir Abbas Bukhari,*[a] Maryam Fatima,[b] Arshad Ali,[c] Tehreem Fatima,[b] Muhammad Ajaz Hussain, [ID] *[b] Haifa Mhaoash Alenzi,[a] Mohamed Abdelwahab Abdelgawad,[a] Mohammad M. Al-Sanea[a] and Naveed Ahmad[d]

The use of polysaccharide-based hydrogels in the development of novel drug delivery systems (DDSs) has increased steadily due to their swellable nature, pH-responsive behavior, biodegradability, biocompatibility, and low toxicity. Arabinoxyan (AX) was obtained using a hot-water extraction approach and esterified with three different concentrations, *i.e.*, 2.5, 5, and 10% of citric acid (CA) in the presence of 4-dimethylaminopyridine (DMAP) as a catalyst to get CA crosslinked AX derivatives (CL-AX-1, CL-AX-2, and CL-AX-3). Fourier transform infrared (FTIR) spectroscopic analysis of AX and CL-AX-2 confirmed the esterification of AX. Scanning electron microscopy (SEM) analysis confirmed the superporous morphology of CL-AX-2, characterized by the presence of interconnected microscopic channels. The CL-AX-2 exhibited stimuli-responsive behavior, with swelling observed in the order: distilled water (DW) > pH 7.4 > pH 6.8 > pH 1.2. The swelling kinetics followed a second-order kinetic model. At pH 6.8, CL-AX-2 sustained the release (92%) of valsartan for up to 24 h, whereas at pH 1.2, nominal drug release (16%) was observed even after 24 h. Valsartan was released using a super case-II transport mechanism and followed first-order kinetics. Moreover, CL-AX-2 appeared to be a biocompatible and non-toxic material and hence highly suitable for sustained/targeted drug delivery.

1 Introduction

Hydrogels are three-dimensional networks of crosslinked polymers that are very useful in mechanical and biological applications because they can absorb a large amount of water without losing their structural integrity. They are widely employed in tissue engineering scaffolds, contact lenses, wound dressings, controlled drug delivery systems, and injectable therapeutic depots because of their high water content, biocompatibility, permeability, and tuneable swelling behavior.[1–4] Applications in regenerative medicine, including the restoration of cartilage, bone, and skin, are made possible by their porous nature, which promotes nutrient transfer and cell proliferation.[5–7] Apart from their biological compatibility, hydrogels have mechanical qualities that may be adjusted, such as elasticity, toughness, compressive strength, and viscoelasticity.[8,9] These properties are obtained by altering the chemical composition, crosslinking density, and adding reinforcing agents. These properties enable their application in wearable sensors, soft robotics, artificial cartilage, load-bearing implants, and flexible bioelectronics.[10,11] Hydrogels are therefore adaptable materials for cutting-edge biomedical and engineering applications due to their blend of biomimetic properties and adjustable mechanical performance. The behavior of hydrogels can be tailored through chemical cross-linking of natural polymers while maintaining the biocompatibility and non-toxicity required for *in vivo* applications.[12,13]

Plantago ovata (syn: psyllium, isabgol, ispaghula, spogel, isapghol) is a commercially important medicinal plant. Its seed husk consists of arabinoxylan-rich, highly branched mucilage polysaccharides that rapidly hydrate in aqueous media to form a viscous gel.[14,15] It is found throughout North Africa, the Mediterranean area, and Asia, particularly in Pakistan and India. *P. ovata* has been extensively used in pharmaceutical, nutraceutical, and functional food applications due to its remarkable water-holding capacity, biocompatibility, and non-toxic nature. The husk of *P. ovata* has been reported to function as a bulk-forming laxative, promoting intestinal motility and normalizing stool consistency in individuals with constipation and irritable bowel syndrome.[16,17] Additionally, its gel-forming soluble fiber supports cardiovascular health by lowering low-density lipoprotein (LDL) cholesterol, improving

[a]*Department of Pharmaceutical Chemistry, College of Pharmacy, Jouf University, Sakaka 72388, Saudi Arabia. E-mail: sbukhari@ju.edu.sa*

[b]*School of Chemistry, University of the Punjab, Lahore 54590, Pakistan. E-mail: majaz172@yahoo.com*

[c]*Institute of Chemistry, University of Sargodha, Sargodha 40100, Pakistan*

[d]*Department of Pharmaceutics, College of Pharmacy, Jouf University, Sakaka 72388, Aljouf, Saudi Arabia*

glycemic management in type-2 diabetes, and reducing post-prandial hyperglycemia.[18–20] Because of its pH-responsiveness, swelling tendency, and capacity to create biodegradable cross-linked networks, *P. ovata* mucilage has been investigated as a natural hydrogel-forming polymer, binder, disintegrant, and controlled-release matrix in material science and drug-delivery research. Collectively, these properties make the *P. ovata* husk a versatile bio-derived material with expanding applications in food technology, biomedical engineering, and pharmaceutical formulations.[21–23]

After being soaked in water, *P. ovata* extruded mucilage, made of arabinoxylan (AX), a hemicellulosic polysaccharide with a well-known structure. AX comprises arabinose side chains with a β-(1 → 4)-linked xylan backbone.[24–26] Biomedical engineers are interested in AX because of its modifiable nature, biodegradability, and availability in plant sources. Furthermore, it has been demonstrated that these AX-based hydrogels react to pH variations, which is particularly useful for drug delivery systems that need environment-triggered release.[27,28]

Hydrogel matrices are often stabilized by chemical cross-linking, which also imparts desired features including decreased solubility, structural integrity, stimuli-sensitive swelling, targeted delivery, and sustained-release performance, thereby emphasizing the relevance and contribution of the present arabinoxylan-based hydrogel system to the evolving field of smart polysaccharide drug delivery materials. Synthetic cross-linkers such as glutaraldehyde, oxalyl chloride, and glyoxal are widely used; however, they are often associated with cytotoxicity, environmental concerns, and significant regulatory challenges. An attractive substitute is citric acid (CA), a naturally occurring, non-toxic, and economical molecule that forms stable cross-linked networks with hydroxyl (–OH) groups in polysaccharide chains.[29–32] The usefulness of CA in developing biocompatible hydrogels has been confirmed by a number of studies. For instance, a CA cross-linked hydroxyethyl tamarind gum film was created and demonstrated to have adjustable mechanical strength, swelling behavior, drug loading, hemocompatibility, and the ability to heal wounds *in vitro*.[33] Similarly, an glucuronoxylans gel system cross-linked with CA showed pH-responsive swelling, reversible swelling-deswelling behavior, and sustained-release of a drug; the hydrogel had a porous superstructure, and the CA cross-linking was verified by FTIR. These achievements highlight the potential of CA as a "green" cross-linker for hydrogels based on polysaccharides.[34]

Thus, cross-linking arabinoxylan (AX) with the green, non-toxic agent such as CA provides a novel hydrogel matrix (CL-AX) that is simultaneously safe for physiological applications and functionally stimuli-responsive. This approach can offer a platform for targeted and sustained drug delivery, enabling controlled release in response to pH changes or other stimuli while minimizing adverse biological effects. The present study aims to synthesize three formulations of CA cross-linked AX (CL-AX) using 2.5% (CL-AX-1), 5% (CL-AX-2), and 10% (CL-AX-3) of CA and to evaluate their stimuli-responsive behavior, structural characteristics using Fourier transform infrared spectroscopy (FTIR), and morphology using scanning electron microscopy (SEM). The aim is to analyze the pH-responsive swelling behavior of CL-AX by conducting stimuli-responsive swelling in buffer systems with varying pH levels, which mimic various physiological levels and swelling-deswelling characteristics. Moreover, the aim is to investigate the drug release using a model drug (valsartan) to assess the release kinetics and mechanism. To ensure the safety of CL-AX for biomedical applications, the hemocompatibility and acute oral toxicity evaluation of CL-AX is also reported herein.

2 Materials and methods

2.1. Materials

The *P. ovata* husk was obtained from Hamdard, Pakistan. After being manually cleaned and sieved, the husk was kept at room temperature in an airtight jar. The $HNO_3 \geq 65\%$, $HCl \geq 37\%$, $NaOH \geq 98\%$, $NaCl \geq 99\%$, $KCl \geq 99\%$, and potassium dihydrogen phosphate ($KH_2PO_4 \geq 99\%$) were all purchased from Riedel-de Haën, Germany, and ethanol ($C_2H_5OH \geq 98\%$) and *n*-hexane (≥95%) were procured from Sigma-Aldrich, USA. BDH (Bristol, England) supplied the tragacanth gum and microcrystalline cellulose (Avicel® PH 101). Acidic and basic buffers were prepared using the procedure outlined in the US Pharmacopeia-National Formulary (USP 34-NF 29). Valsartan, a USP-standard drug, served as a model to assess the synthesized hydrogel for the sustained release of the drug. Before being cleaned with distilled water (DW), glassware was rinsed with HNO_3. Additionally, dilutions and required solutions were prepared using the DW.

2.2. Isolation of hydrogel

Psyllium hydrogel/arabinoxylan (AX) was isolated using an alkali-extraction method.[23] Briefly, psyllium husk (100 g) was soaked in DW for 24 h at a husk-to-water ratio of 1 : 50 (w/v). The pH of the suspension was adjusted and maintained at 12 by the gradual addition of 2.5% (w/v) NaOH solution to facilitate efficient extraction. Vacuum filtration was used to separate the AX. Later, glacial acetic acid was used to keep the pH at 3 to coagulate AX. After de-fatting, the AX with *n*-hexane and AX was washed with DW up to neutral pH. The AX hydrogel was then centrifuged, air-dried on glass sheets, ground into a powder, passed through sieve number 60, and kept in an airtight container in a desiccator.

2.3. Synthesis of CL-AX-2

A reported procedure[31] was applied with minor amendments to crosslink the AX with CA. Briefly, AX (2 g) was dispersed in 50 mL of DMAc and stirred at 100 °C for 2 h to obtain a hydrogel-like suspension. In parallel, CA (5 g) was dissolved in 100 mL of DW to prepare a 5% (w/v) solution, which was subsequently added to the AX-DMAc suspension. The crosslinking reaction was catalyzed with DMAP (50 mg) and maintained at 100 °C for 24 h. The resulting CA-crosslinked AX (CL-AX-2) was precipitated in 150 mL of methanol, thoroughly washed with DW, vacuum-dried at 60 °C, and ground into a fine powder. The dried material was stored in a vacuum-sealed container until further use. CL-AX-1 and CL-AX-3 were synthesized following

the same protocol using 2.5% and 10% CA, respectively. Based on preliminary evaluation of experimental yield, degree of substitution (DS), and equilibrium swelling in DW, the formulation containing 5% CA (CL-AX-2) demonstrated optimal performance and was therefore selected and scaled up for subsequent investigations.

Yield: CL-AX-1 = 68%, CL-AX-2 = 81%, and CL-AX-3 = 76%

Degree of CA-substitution (DS): CL-AX-1 = 1.87, CL-AX-2 = 2.1, CL-AX-3 = 1.93

FTIR (KBr, cm^{-1}): AX: 3363 (–OH), 2935 (–CH, –CH$_2$), 1610 (C–O), 1018 (COC$_{Ether}$)

CL-AX-2: 3386 (–OH), 2929 (–CH, –CH$_2$), 1724 (C=O$_{Ester}$), 1037 (COC)

2.4. Characterization

FTIR spectra of AX, CA, and CL-AX-2 were obtained using an IR Prestige-20 spectrometer (Shimadzu, Japan) in transmission mode after preparing KBr pellets of the samples. To prepare a clear pellet with a diameter of 13 mm, the mixture was put into a pellet die and compressed for 1–3 min under a force of 5–10 tons, and the obtained pellets were dried in a vacuum oven at 50 °C to eliminate adsorbed moisture before analysis.

The sample, CL-AX-2, was first freeze-dried, and then tiny fragments (about 3–5 mm) of it were adhered to aluminum stubs using conductive carbon tape. Au/Pd was sputter-coated onto the samples to a thickness of around 3–8 nm. Scanning electron microscopy (SEM) was employed to examine surface morphology. The instrument was operated under high-vacuum conditions using a secondary electron detector, with an accelerating voltage of 1–5 kV and a working distance of 5–10 mm to obtain detailed micrographs.

2.5. Flow-ability parameters

The capacity of any material to flow determines its suitability as a pharmaceutical excipient. To determine the flow properties of CL-AX-2 to use it as a pharmaceutical excipient, several flow–ability parameters, including the angle of repose (θ), bulk density (Db), tapped density (Dt), Carr's index (C$_i$), and Hausner ratio (Hr), were calculated (SI, S2.5).

2.6. Stimuli-responsive swelling properties

The swelling behavior of CL-AX-2 was investigated in DW and buffer solutions at pH 1.2, 6.8, and 7.4 using a tea-bag gravimetric method.[35,36] Accurately weighed samples (100 mg) of dried CL-AX-2 were placed into individual tea bags, sealed, and immersed in the respective swelling media at room temperature. At predetermined intervals, the tea bags were withdrawn and suspended briefly to allow excess surface liquid to drain prior to further measurements. The tea bags with swollen CL-AX-2 were then weighed, and using eqn (1), the swelling capacity (g g^{-1}) in each swelling medium was determined.

$$\text{Swelling capacity} (\text{g g}^{-1}) = \frac{W_s - W_i - W_e}{W_i} \quad (1)$$

where, W_i is the weight (g) of CL-AX-2 packed in the tea bags for swelling experiments, W_e is the weight (g) of the tea bag before packing CL-AX-2, and W_s is the weight (g) of the wet tea bag containing sample in swollen form.

Equilibrium swelling of CL-AX-2 in each medium was determined following the same procedure described above. Briefly, an accurately weighed sample was enclosed in tea bags and immersed in the respective swelling media for 24 h to reach equilibrium. The equilibrium swelling capacity was then calculated according to eqn (1).

2.7. Swelling kinetics

Swelling data obtained for CL-AX-2 in DW and buffer solutions at different physiological pH values were further analyzed to determine the extent of swelling and the kinetics of water uptake. For this analysis, the normalized degree of swelling (Q_t) and the normalized equilibrium degree of swelling (Q_e) were calculated using eqn (2) and (3), respectively.

$$Q_t = \frac{W_s - W_d}{W_d} = \frac{W_t}{W_d} \quad (2)$$

$$Q_e = \frac{W_\infty - W_d}{W_d} = \frac{W_e}{W_d} \quad (3)$$

where, W_s denoted the weight of the swelled CL-AX-2 enclosed in wet tea bag at any time t, W_d indicated the weight of CL-AX-2 in dried form at time $t = 0$, W_t represents the weight of water/buffer trapped in the CL-AX-2 from the swelling media at any time t, W_∞ is the weight of the wet tea bag with swelled CL-AX-2 at any time t_∞, meaning that swelling equilibrium is reached.

The values of Q_t and Q_e were further fitted to the second-order swelling kinetic model using the given below (eqn (4)) linearized equation.

$$\frac{t}{Q_t} = \frac{t}{Q_e} + \frac{1}{kQ_e^2} \quad (4)$$

where, k represents the kinetic constant of the second-order model and was determined from the intercept of the linear regression plot of t/Q_t versus t. The applicability of the second-order kinetic model to the swelling data was assessed using the correlation coefficient (R^2), and the model with the highest R^2 value was considered to provide the most appropriate description of the swelling behavior of CL-AX-2.

2.8. Effect of electrolytic stress on the swelling

The amounts of salts in the solution also influence the swelling potential of any hydrogel system, in addition to pH. To prove CL-AX-2 as a salt-responsive candidate for the drug delivery applications, solutions of different molar concentrations (0.1, 0.5, 1.0, 1.5, 2, 3, and 4 M) of salts such as NaCl and KCl were prepared in DW. The tea bag with 100 mg of CL-AX-2 was submerged in each salt solution for 24 h. The tea bags were removed from the aqueous salt solution after 24 h, and their weight was determined using eqn (1) for swelling capacity.

2.9. On-off switching properties

The swelling and deswelling (on-off switching) studies for CL-AX-2 were performed in the buffer of pH 7.4 (swelling medium) and buffer of pH 1.2 (deswelling medium), DW (swelling medium) and ethanol (deswelling medium), and DW and 0.9% aq. solution of NaCl (deswelling medium) for the assessment of CL-AX-2 as a stimuli-responsive material. For the swelling–deswelling study, 100 mg of CL-AX-2 was placed in a pre-weighed tea bag, sealed, and immersed in a pH 7.4 buffer at room temperature. The tea bag was removed at 15 min intervals, and the swelling capacity was determined using eqn (1). After 1 h, the swollen sample was transferred to a deswelling medium (pH 1.2 buffer) and maintained for an additional hour to evaluate deswelling behavior. Reproducibility was examined through four consecutive swelling-deswelling on-off cycles. The switching response of CL-AX-2 was further assessed in DW/ethanol and DW/normal saline systems following the same experimental protocol.

2.10. Development of CL-AX-2 as a sustained-release material

2.10.1. Preparation of CL-AX-2 and valsartan-based tablets.

The suitability of CL-AX-2 as a sustained-release excipient was investigated through tablet formulation using valsartan as a model drug, which was prepared by a wet granulation technique.[37] Briefly, CL-AX-2 (300 mg) and valsartan (100 mg) were blended thoroughly in a mortar and pestle. A sufficient quantity of 5% (w/v) polyvinylpyrrolidone solution in isopropyl alcohol was then added as a granulating agent to form a cohesive damp mass. The wet mass was dried and passed through sieve No. 16 to obtain uniform granules. The granules were subsequently lubricated with magnesium stearate (20 mg) and compressed into tablets using a single-punch tablet press and resulting tablets exhibited an average diameter of 9 mm, thickness of 4.5 mm, and hardness of 6.5 kg cm^{-2}.

2.10.2. *In vitro* valsartan release study.

The *in vitro* release of valsartan from CL-AX-2-based tablets was evaluated in buffer solutions at pH 1.2 and 6.8, simulating the gastric and intestinal environments, respectively. The study was conducted using a USP Dissolution Apparatus II, with the dissolution media maintained at 37 °C and the paddle rotating at 50 rpm. At predetermined time intervals, 5 mL aliquots were withdrawn, filtered, and diluted as necessary, and the amount of released drug was quantified by measuring absorbance at 249 nm using a UV-vis spectrophotometer. Drug concentrations were determined from a previously constructed calibration curve. Additionally, the dissolution profile of valsartan at pH 6.8 was recorded for comparative analysis.

2.10.3. Valsartan release kinetics.

The rate and extent of the drug released during the dissolution/release study were monitored through kinetic models. Therefore, first-order kinetics[38] and the Korsmeyer–Peppas model[39] were used to evaluate the drug release kinetics and mechanism using eqn (5) and (6), respectively.

$$\log Q = \log Q_0 - \left(\frac{K_1 t}{2.303}\right) \tag{5}$$

$$\frac{M_t}{M_\infty} = k_p t^n \tag{6}$$

where, the amount of the drug that has to be released after time t, and the initial amount of drug loaded are represented by Q and Q_0, respectively. The rate constants for the first-order and Korsmeyer–Peppas models are represented by K_1 and k_p, respectively. The amount of drug release after time t and the diffusion exponent are represented by M_t/M_∞ and n, respectively. Using the value of n, the drug release mechanism can be elucidated. The value of n can be ≤ 0.45, between 0.45 and 0.89, equal to 0.89, and > 0.89 for Fickian diffusion, non-Fickian diffusion, case-II transport, and super case-II transport mechanism.[39,40]

2.11. Haemocompatibility studies

Hemolytic potential and thrombogenicity tests of CL-AX-2 were conducted in accordance with the International Standard Organization's (ISO) standard operating procedures.[41]

2.11.1. Hemolytic potential.

Following the American Society for Testing and Materials (ASTM) protocol as reported elsewhere,[42] the hemolytic potential was assessed to monitor any unfavorable interaction of CL-AX-2 with the blood.

A sample of CL-AX-2 (500 mg) was first soaked in phosphate-buffered saline (PBS) for 24 h at 37 °C ± 0.5 °C. It was then incubated for 3 h at the same temperature with a known concentration of citrated blood. Following incubation, the mixture was centrifuged at 10^4 rpm for 15 min, and the supernatant was collected. The optical density (OD) of the supernatant was measured at 540 nm using a UV-vis spectrophotometer.[43] A known quantity of citrate blood and water was utilized as the positive control, and citrate blood and PBS were used as the negative control. Eqn (7) was used to determine the hemolytic potential.

Hemolytic index (%) =
$$\frac{\text{OD of test sample} - \text{OD of }(-)\text{ control}}{\text{OD of }(+)\text{ control} - \text{OD of }(-)\text{ control}} \times 100 \tag{7}$$

2.11.2. Thrombogenicity.

The gravimetric method was used to assess the thrombogenicity potential of CL-AX-2. Precisely weighed CL-AX-2 (500 mg) was soaked in PBS for 24 h at 37 °C ± 0.5. After decanting the surplus PBS, 2 mL of citrate blood and 0.2 mL of CaCl$_2$ (0.1 M) were added. For 45 min, the mixture was put aside, followed by the addition of DW to prevent the blood from clotting. The clots were fixed with formaldehyde (36–38%, 5 mL), dried, and weighed.[31] The same process was used without CL-AX-2 for the positive control, and without CL-AX-2 and blood for the negative control. Eqn (8) was used to determine the thrombogenicity.

Thrombose(%) =
$$\frac{\text{Mass of test sample} - \text{mass of }(-)\text{ control}}{\text{Mass of }(+)\text{ control} - \text{mass of }(-)\text{ control}} \times 100 \tag{8}$$

2.12. Acute oral toxicity evaluation

Acute oral toxicity testing of CL-AX-2 was conducted in accordance with the guidelines presented in the National Institutes of Health (NIH) Handbook for the Care and Use of Laboratory Animals (NIH Publication No. 8023, revised 1978) and the Organization for Economic Co-operation and Development (OECD) Guideline 420.[44,45] For this study, rabbits were procured from the animal facility of The University of Lahore, Pakistan. The animals were maintained in clean cages under controlled conditions, including a temperature of 22–25 °C, 50% relative humidity, and a 12 h light–dark cycle. They were provided with ad libitum access to water and a standard laboratory diet. Three dosages of CL-AX-2 (0.03 g per kg body weight (bw), 0.5 g per kg bw, and 2 g per kg bw were administered once at the start of the study to three different groups of animals ($n = 5$ in each group). Whereas the animals of a control group did not receive any dose of CL-AX-2. The University of Lahore Institutional Research Ethics Committee authorized the experimental procedures in letter number IREC-2018-76 M, dated May 17, 2018. Daily measurements of body weight, food, and water intake were taken during acute oral toxicity investigations. Along with indications of allergies, diarrhoea, altered reflexes, tremors, and salivation, animals were also observed for any potential toxicity indicators. After 14 days, the blood samples were taken by heart puncture for hematological and biochemical analyses, including complete blood counts, lipid profiles, liver function tests, uric acid testing, and renal function tests. To determine the absolute organ weight, the animals were sacrificed, and the vital organs such as the liver, large intestine, stomach, spleen, kidney, lungs, and heart were removed and weighed. Histological examination was carried out to examine the tissue integrity of essential organs and to evaluate some important criteria, such as degeneration, leukocyte infiltration, necrosis, fibrosis, and blood extravasation. Vital organs were preserved in 10% formalin, cut into 5 mm-thick sections, stained with hematoxylin-eosin dye, and inspected under a light microscope.

The acute dermal and eye irritation tests were also performed using OECD guideline 402 and the Draize scale, respectively.[46,47]

All the experiments were conducted in triplicate and the average of the values are presented here.

3 Results and discussion

3.1. Isolation of AX and synthesis of CL-AX

The AX was extracted through the alkali extraction method, and its yield was found to be 19.8%. The process for the crosslinking of AX with CA to synthesize CL-AX is shown in Fig. 1. While heating the reaction mixture, at 80 °C, CA dehydrates from one side and changes into the more reactive cyclic anhydride-I form, which then reacts with –OH of AX to synthesize AX-citrate. *In situ*, the second terminal of CA will likewise transform into cyclic anhydride-II. This cyclic anhydride-II reacts further with any other available AX unit to cross-link it, producing CL-AX.

3.2. Preliminary swelling studies and optimization of ideal formulation

Three different concentrations of CA (as a cross-linking agent), *i.e.*, 2.5, 5, and 10%, w/v, were used to synthesize three different CL-AX derivatives, *i.e.*, CL-AX-1, CL-AX-2, and CL-AX-3. The experimental yield of CL-AX-1, CL-AX-2, and CL-AX-3 was found to be 68, 81, and 76%, respectively. The degree of substitution of citrate moieties on the polymeric backbone of AX was calculated according to acid–base titration method[48] and found to be 1.87, 2.1, and 1.93. The equilibrium swelling capacity graph of CL-AX-1, CL-AX-2, and CL-AX-3 is shown in Fig. 2. The equilibrium swelling of CL-AX-1, CL-AX-2, and CL-AX-3 was found to be 18, 26, and 24 g g^{-1} after 24 h (Fig. 2). Therefore, due to high experimental yield, DS, and equilibrium swelling in DW, the formulation CL-AX-2 prepared using the 5% of CA was found to be the best one. Hence, CL-AX-2 was further used for the evaluation of physicochemical properties and for drug delivery applications.
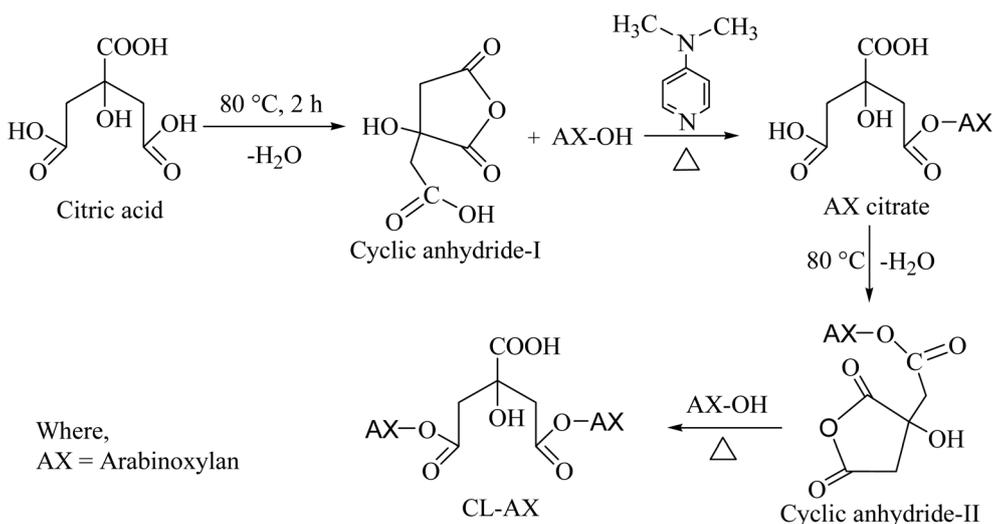

Fig. 1 Schematic representation of the stepwise conversion of arabinoxylan (AX) into cross-linked AX (CL-AX) using citric acid (CA).
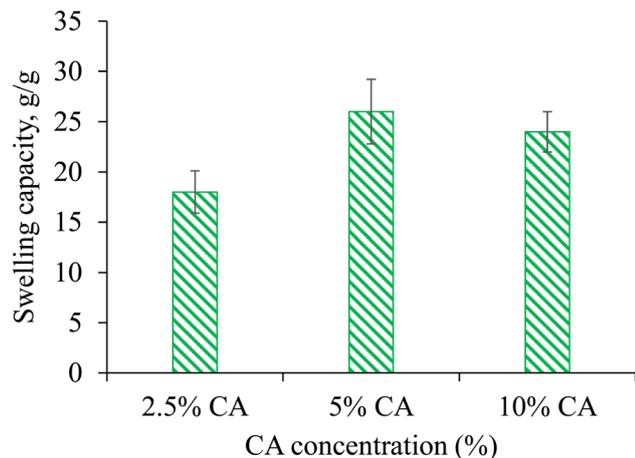
Fig. 2 Equilibrium swelling of CL-AX prepared using 2.5% (CL-AX-1), 5% (CL-AX-2), and 10% (CL-AX-3) of CA concentration in DW.

3.3. Characterization

3.3.1. FTIR analysis. The FT-IR spectra of AX, CA, and CL-AX-2 (Fig. 3) were recorded to determine the location of the absorption bands and the key functional groups present in the AX before and after crosslinking. The hydroxyl (–OH) functionalities of the repeating glycosidic units appeared at 3363 and 3386 cm^{-1} and C–H at 2935 and 2929 cm^{-1} for AX and CL-AX-2, respectively. The most valuable ester peak (incorporation of a new functional group) appeared at 1724 cm^{-1} in CL-AX-2, indicating the success of the esterification reaction.[31] After crosslinking, the OH band moves from 3363 to 3386 cm^{-1}, showing that some hydroxyl groups reacted to form ester linkages and the original strong polymer–polymer hydrogen bonding decreased. The wider OH peak indicates new interactions forming between the remaining –OH groups and the carbonyl groups of CA. Overall, this suggests that the hydrogen-

bonding network becomes reorganized and slightly weaker within the crosslinked polymer structure.[31] For comparison, the FTIR spectrum of CA is provided (Fig. S1).

3.3.2. SEM analysis. The surface morphology of CL-AX-2 was examined using SEM micrographs of its transverse and longitudinal cross-sections. The images revealed the internal channel architecture as well as the overall textural features of CL-AX-2. The surface exhibited well-distributed macropores and interconnected channels (Fig. 4(a and c)). Image analysis was performed to generate histograms of pore size distribution, plotting percentage frequency *versus* pore diameter. The average pore diameters were determined to be 5.1 ± 2.3 μm for transverse cross-sections and 5.3 ± 2.4 μm for longitudinal cross-sections (Fig. 4(b and d)). The presence of well-distributed macropores and interconnected channels suggests that CL-AX-2 can efficiently absorb biological fluids, highlighting its potential as a hydrogel matrix for controlled drug delivery.

3.4. Physical and flow properties

The physical properties and flowability of CL-AX-2 are summarized in Table 1. An angle of repose of 39.21 ± 3.14° indicates passable flow, while the Hausner ratio (1.322 ± 0.74) and Carr's index (26.8 ± 2.3%) point to poor flowability. Thus, improving flow properties is recommended before formulating CL-AX-2-based tablets. When used as an excipient, strategies such as wet or dry granulation and the addition of appropriate lubricants or glidants can optimize handling and processing.

3.5. Stimuli-responsive swelling studies

To evaluate the potential of CL-AX-2 as a pH-responsive, swellable material for sustained-release drug delivery, its dynamic swelling behavior was assessed in DW and buffers at pH 1.2, 6.8, and 7.4. As shown in Fig. 5(a), CL-AX-2 showed the highest swelling in DW, followed by buffers at pH 7.4 and 6.8, whereas nominal swelling was observed at pH 1.2. The increased
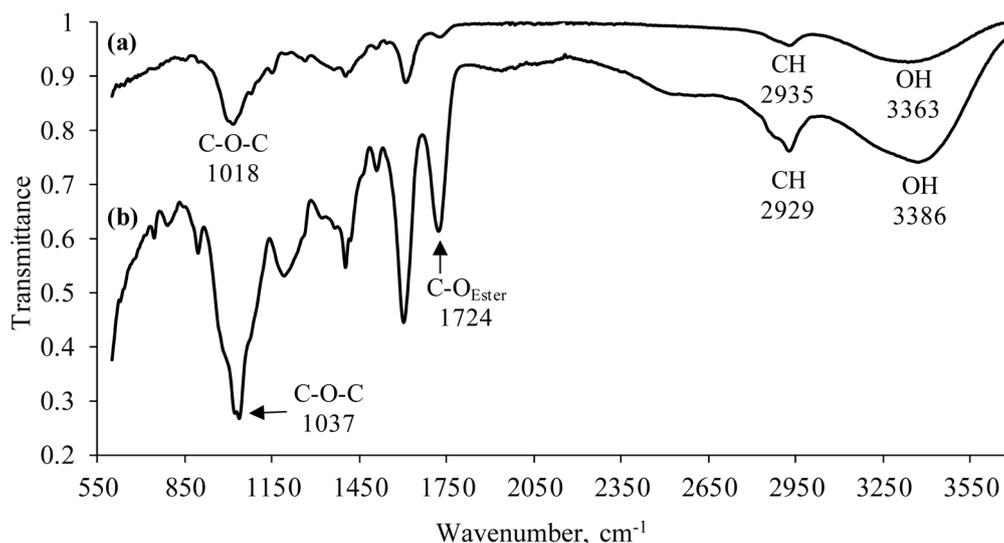

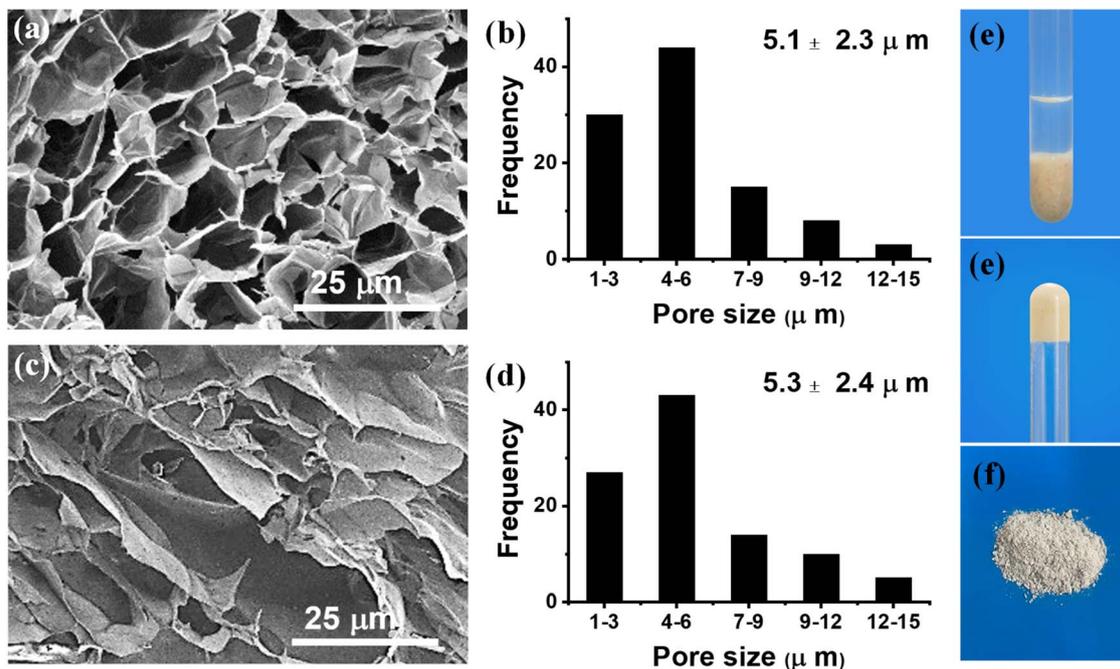Fig. 3 FTIR spectra of AX (a) and CL-AX-2 (b).

Fig. 4 Transverse (a) and longitudinal (c) cross-sectional SEM images of CL-AX-2, with the corresponding pore size distribution histograms (b and d), respectively. The physical appearance of CL-AX-2 in its hydrogel (e) and powdered (f) forms is also shown.

Table 1 Physical properties and flowability parameters of CL-AX-2

Properties	CL-AX-2
Moisture content (%)	7.2 ± 0.6
Loss on drying (%)	5.9 ± 0.7
Angle of repose (°)	39.21 ± 3.14
Bulk density (g cm^{-3})	0.413 ± 0.057
Tapped density (g cm^{-3})	0.504 ± 0.046
Carr's index (%)	26.8 ± 2.3
Hausner ratio	1.322 ± 0.74
Swelling capacity (g g^{-1}) in DW after 24 h	26 ± 2.12

swelling at pH 6.8 and 7.4 is attributed to the deprotonation of carboxylic acid (–COOH) groups to carboxylate ions (–COO$^-$), which induces electrostatic repulsion and relaxation of the polymer network.[29] The higher swelling in DW, compared to buffer solutions, is likely due to the absence of charge-screening ions such as Na$^+$ and K$^+$. Conversely, at pH 1.2, the –COOH groups remain largely protonated, keeping the polymer chains tightly packed and restricting buffer penetration.[20] These results indicate that CL-AX-2 is a swellable, pH-sensitive material suitable for developing pH-dependent drug delivery systems.

3.6. Swelling kinetics

The experimental swelling data were fitted to different kinetic models in order to have a better understanding of the swelling mechanism. The swelling data fitted well to the second-order swelling kinetic model among the investigated models because of the higher value of regression coefficients, *i.e.*, $R^2 \geq$
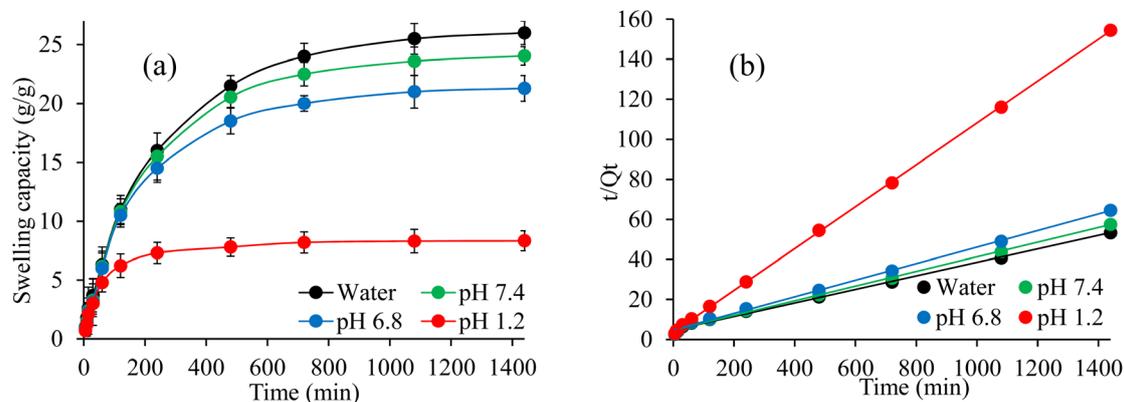

Fig. 5 Dynamic swelling of CL-AX-2 (a) and swelling kinetics of CL-AX-2 (b) in DW and at pH 1.2, 6.8, and 7.4 (b) for 1440 min (24 h).

0.99 (Fig. 5(b)). The high linearity of the plot between t/Q_t vs. t indicated that the swelling process of CL-AX-2 is not governed solely by Fickian diffusion, but also influenced by polymer chain relaxation and polymer–solvent interactions.[39,40] The observed second-order swelling behavior is particularly beneficial from a drug delivery perspective since it shows a controlled and predictable swelling mechanism. By avoiding premature burst release, gradual swelling controlled by polymer relaxation can enhance drug entrapment effectiveness and promote prolonged drug release. Consequently, the swelling kinetics of the current hydrogel system validate its appropriateness for site-specific and controlled drug delivery applications. Similar swelling behaviour has been reported in the literature for polysaccharide-based pH-responsive hydrogel systems where solvent diffusion and chain relaxation mechanisms occur.[23,32,36]

3.7. Saline-responsive swelling

To evaluate the impact of salts on the swelling behavior of CL-AX-2, its equilibrium swelling (after 24 h) was measured in NaCl and KCl solutions of varying molarity (0.1–4 M). The results demonstrated that the swelling of CL-AX-2 was dependent on the ionic strength of the salt solutions, showing distinct responses with increasing concentrations of NaCl and KCl. Upon increasing the salt concentration from 0.1–0.5 M, a pronounced reduction in swelling was observed (Fig. 6(a)). This behavior can be attributed to the presence of monovalent ions, such as Na$^+$ and K$^+$, which diminish electrostatic repulsion

among ionized carboxylate groups by neutralizing their charges, thereby restricting polymer chain expansion. At higher salt concentrations (1–4 M), the swelling of CL-AX-2 increased again. Under these conditions, strong ion–polymer interactions and partial weakening of intermolecular hydrogen bonding may enhance polymer chain mobility, allowing greater water uptake. In addition, the elevated ionic strength creates a concentration gradient that favors solvent diffusion into the hydrogel network. Moreover, the recovery of swelling of CL-AX-2 at higher concentrations of salts, i.e., from 1–4 M, can be better explained from a thermodynamic perspective based on polyelectrolyte hydrogel theory. According to this theory, when external electrolytes are present, the osmotic pressure differential between the hydrogel network and the surrounding fluid is decreased by charge screening at low to moderate ionic strength, which results in less swelling. Nevertheless, the screening effect becomes almost saturated at extremely high salt concentrations, and more counter-ions start to take part in the development of ion pairs with the ionizable groups of the polymer network. This ion-pairing weakens inter- and intra-chain hydrogen bonding and partially disrupts secondary physical crosslinks, thereby increasing chain mobility and free volume within the network.[49] Additionally, the Donnan equilibrium theory states that the equilibrium swelling is determined by the balance between the ionic osmotic pressure and the elastic retractive forces of hydrogel networks. Despite overall charge screening, some re-expansion (swelling recovery) of the network
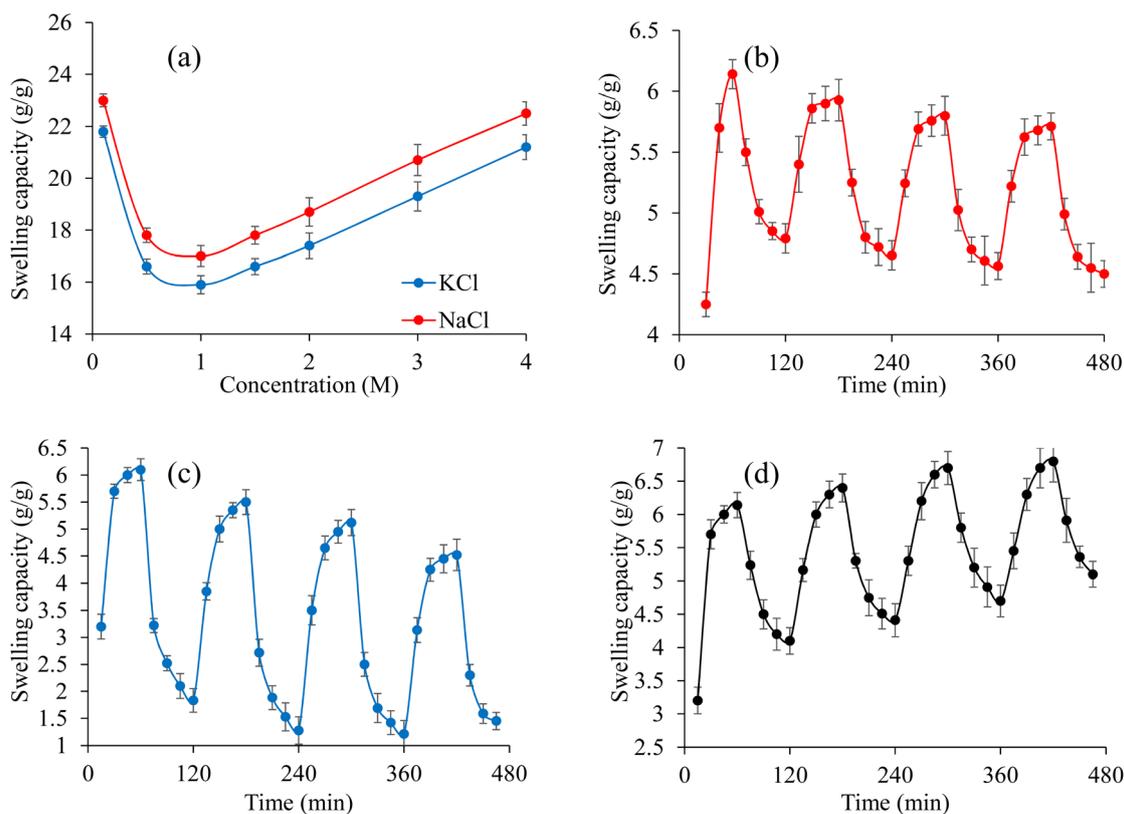

Fig. 6 Swelling of CL-AX-2 in NaCl and KCl solutions of different molar concentrations after 24 h (a) and swelling–deswelling of CL-AX-2 at pH 7.4 and 1.2 (b), DW and ethanol (c), and DW and saline (d).

occurs at high ionic strength due to the dynamic exchange of counter-ions between the external solution and the fixed charges of the hydrogel, which strengthens ionic-polymer connections. The observed rise in swelling at high salt concentrations is explained by the combined effects of saturated electrostatic screening, ion-pair creation, and secondary interaction relaxation.[50]

3.8. On-off switching properties

The on-off switching characteristics of CL-AX-2 were demonstrated by its response in the pH 7.4 and 1.2 buffer. Fig. 6(b) incorporates the findings of CL-AX-2 swelling and deswelling at pH 7.4 and 1.2, respectively. As can be observed, the CL-AX-2 rapidly swelled in the pH 7.4 buffer (recorded for 1 h), and it deswelled when transferred to the pH 1.2 buffer. The swelling process began at pH 7.4 when the –COOH groups in the CL-AX-2 ionized to –COO$^-$ and anions began to repel one another electrostatically. However, in the pH 1.2 buffer, the deswelling process of CL-AX-2 was initiated by the re-conversion of –COO$^-$ to –COOH, *i.e.*, un-ionized form after obtaining a proton from the acidic environment of the pH 1.2 buffer; hence, CL-AX-2 deswells. The four cycles of swelling and deswelling were recorded to examine the consistency and reproducibility of the on-off switching characteristics of CL-AX-2 at pH 7.4 and 1.2. Almost identical behavior was noted.

In DW, CL-AX-2 exhibited rapid swelling; however, upon transfer to ethanol as the deswelling medium, a pronounced reduction in swelling was observed (Fig. 6(c)). This reversible swelling–deswelling behavior can be attributed to the substantial difference in polarity and dielectric constants of the two solvents. DW, with a high dielectric constant (80.40), promotes polymer chain expansion through strong hydration, whereas ethanol, having a much lower dielectric constant (24.55), limits solvent–polymer interactions and induces network contraction. The alternating swelling and deswelling response remained consistent over four successive cycles, demonstrating the reversible nature of the system. As solvent polarity can influence hydrogel swelling and, consequently, drug release behavior, caution may be warranted regarding the concurrent intake of alcohol-containing beverages during treatment with CL-AX-2-based formulations.[51] It is noteworthy that these results dealt with ethanol sensitivity of the hydrogel system only under elevated ethanol concentrations, and that further systematic studies across physiologically relevant ethanol levels are required to establish a definitive threshold at which ethanol significantly affects drug release.

A similar on-off swelling response was observed when DW and normal saline were used as the swelling and deswelling media, respectively (Fig. 6(d)). CL-AX-2 swelled rapidly in DW, while exposure to saline resulted in deswelling due to charge-screening effects caused by dissolved ions. This reversible behavior persisted over four cycles, confirming the saline-responsive nature of CL-AX-2. Concludingly, it can be stated that these findings support the on-off switching capability of CL-AX-2 and its suitability as a stimuli-responsive hydrogel for controlled drug delivery applications.

3.9. *In vitro* valsartan release studies

The results of the valsartan release study are presented in Fig. 7. CL-AX-2 effectively sustained the release of valsartan for 24 h at pH 6.8, with approximately 92% of the drug released, whereas only 16% was released at pH 1.2. Notably, CL-AX-2 largely restricted valsartan release under acidic conditions (pH 1.2). These findings suggest that CL-AX-2 is suitable for sustained intestinal delivery of valsartan over 24 h, while minimizing drug release in the stomach environment.

After calculating the release kinetics and release mechanism from valsartan release data, it was observed that the valsartan release followed the first-order kinetics as the value of the $R^2 = 0.9742$ is approaching "1". Similarly, the value of R^2 and n for the Korsmeyer–Peppas model is recoded as 0.9928 and 0.595, respectively, indicating the best fit model and following the non-Fickian diffusion mechanism for valsartan release.[39]

3.10. Haemocompatibility studies

The hemolytic index of CL-AX-2 was 4.65 ± 0.08%, and the thrombosis value was 89.73 ± 3.27%. The American Society for Testing and substance's ASTM F 756–00 safety regulations state that a substance is hemolytic in nature if its hemolytic index value is less than 5%, which makes it safe for use in biomedical applications. Likewise, a substance is considered non-thrombogenic if its thrombogenicity rating is less than 100%. As a result, CL-AX-2 is a substance that is safe for use in biomedical applications.[42]

3.11. Acute oral toxicity studies

The animals from the treatment groups were determined to be active and healthy after the 14 days acute oral toxicity study. Throughout the whole research, no behavioural changes were noted. Additionally, no side effects, such as skin rashes, tremor, diarrhea, constipation, or allergic reactions, were noted, which indicated the non-toxic nature of CL-AX-2.

Throughout the whole research period, the animals from all treatment groups consumed less food. The delay might be caused by the presence of swellable material in the GIT. The
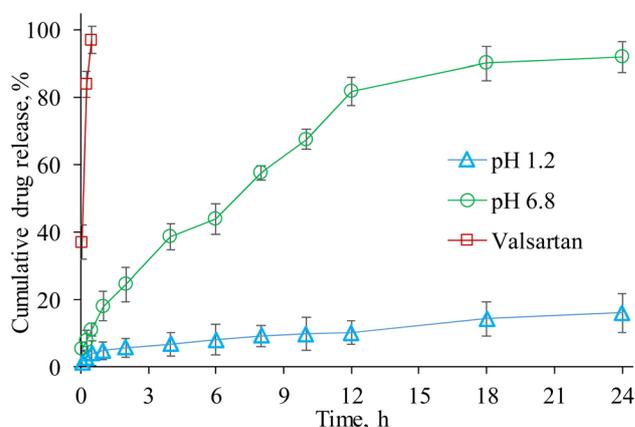

Fig. 7 Valsartan release from CL-AX-2-based tablets at pH 1.2 and 6.8 and the release of the control drug sample at pH 6.8.

Table 2 Hematological parameters of rabbits

Parameters	Group "I"	Group "II"	Group "III"	Group "IV"
TLC ($\times 10^3$ μL^{-1})	5.92	7.13	6.32	7.04
RBC ($\times 10^6$ μL^{-1})	6.18	7.60	6.51	5.49
Hb (g dL^{-1})	10.7	11.29	10.41	11.32
HCT (PCV) (%)	36.3	35.5	38.29	34.7
MCV (fL)	67.2	72.1	75.4	69.0
MCH (pg)	20.1	22.41	25.3	21.5
MCHC (g dL^{-1})	30.5	31.7	29.8	33.1
Platelet count ($\times 10^3$ μL^{-1})	272.3	265.1	248.2	259.7
Neutrophils (%)	67.4	66.7	69.1	63.9
Lymphocytes (%)	28.6	29.3	27.2	32.5
Monocytes (%)	1.9	1.3	1.7	1.1
Eosinophils (%)	2.1	2.7	2.0	2.5

empty period of the stomach decreases hunger, leading to decreased food consumption and weight reduction. Throughout the whole study period, there was no discernible change between the treated and untreated animals' bodyweight, water intake, or food intake. On days 3 and 5, however, there was a noticeable difference in the animals' body weight between groups III and IV. After consuming CL-AX-2 for a longer period of time, the desire or yearning to eat decreased, which eventually affected the body weight of the animals. Similarly, a significant difference in the food consumption of animals of groups III and IV was also observed on day 14 (Tables S1 and S2).

The absolute organ weight values of rabbits were obtained (Table S3) and revealed a negligible change compared to the control. The hematological and biochemical parameters of rabbits were determined to be within normal limits and comparable to those of the animals in the control group (Table 2). A negligible difference was found in the levels of serum electrolytes, erythrocyte sedimentation rate, liver function and renal function tests, and complete blood count. However, animals in group IV showed a significant difference in the levels of cholesterol, triglycerides, and low-density lipoprotein (LDL). Consequently, regular CL-AX-2 consumption can lower cholesterol, triglyceride, and LDL concentrations, hence lowering the risk of cardiovascular diseases (Table 3). These findings suggest a promising ancillary application in weight management and lipid profile modulation. However, further targeted studies

Table 3 Biochemical parameters of rabbits

| Parameters	Group "I"	Group "II"	Group "III"	Group "IV"
Lipid profile				
Cholesterol (mg dL^{-1})	132.2	139.0	129.4	135.1
Triglyceride (mg dL^{-1})	124.1	127.5	121.0	120.3
HDL (mg dL^{-1})	44.7	43.6	46.1	49.2
LDL (mg dL^{-1})	63	61.2	69	65.3
VLDL (mg dL^{-1})	23.4	25.1	23.7	24.5
Liver function test				
Bilirubin (mg dL^{-1})	0.6	0.9	0.6	0.8
SGPT (ALT) (U L^{-1})	144.5	142.4	139.8	141.7
SGOT (AST) (U L^{-1})	157.3	163.1	154.6	161.0
ALP (U L^{-1})	119.2	112.7	115	111.5
Total protein (g dL^{-1})	5.8	5.7	6.2	6.9
Albumin (g dL^{-1})	2.0	2.1	2.3	2.6
Globulin (g dL^{-1})	1.9	1.7	2.0	2.3
A/G ratio	1.05	1.24	1.15	1.13
Renal function test				
Urea (mg dL^{-1})	44.3	52.8	51.6	48.2
Creatinine (mg dL^{-1})	1.1	1.5	1.4	1.3
Uric acid (mg dL^{-1})	3.3	3.9	3.7	4.0
Hematology				
ESR (mm h^{-1})	2.6	3.1	2.4	2.9
Serum electrolyte				
Potassium (mmol L^{-1})	3.8	3.2	2.9	3.6
Sodium (mmol L^{-1})	135.1	131.2	137.5	139.3
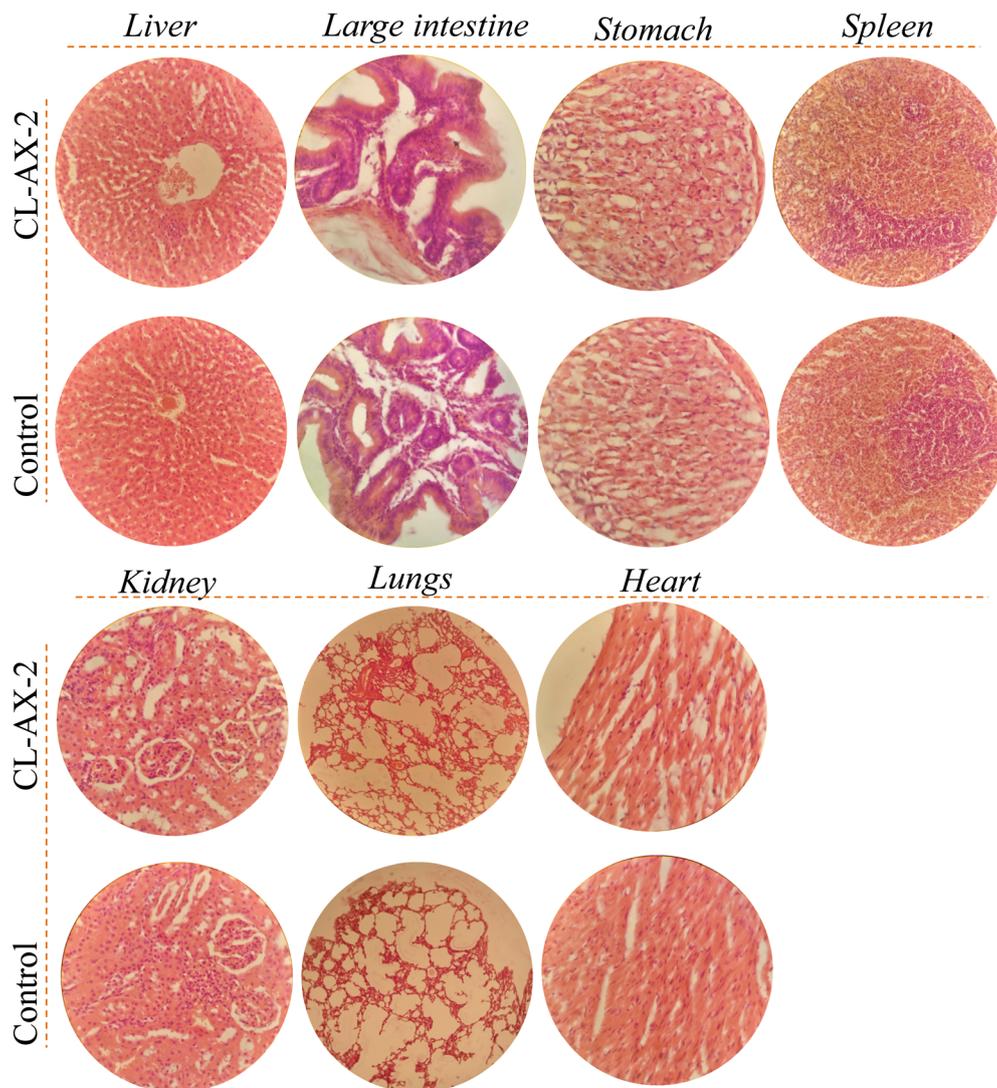
Fig. 8 Histopathology of vital body organs of rabbits.

would be necessary to systematically evaluate the efficacy, dosage, and safety of such applications before any clinical translation.

Throughout the histopathological examinations, the potentially harmful effects of CL-AX-2 on the cellular architecture of the rabbit's important organs were assessed. Histological examination of the heart, kidney, liver, stomach tissues, large intestine, spleen, and lungs is expressed in Fig. 8. Furthermore, the histology of all essential organs showed no evidence of inflammation, necrosis, bleeding, or lesions. As a result, CL-AX-2 can be used for a longer time without harming the tissues of important organs.

4 Conclusion

Citric acid cross-linked arabinoxylan hydrogels (CL-AX) are a potential class of biopolymeric materials for drug delivery and biological applications, as the current study effectively proved. The –OH groups of AX could create persistent ester connections with

CA, an effective, environmentally friendly, and non-toxic/green cross-linker that produced a strong three-dimensional network. The successful formation of the CL-AX-2, enhanced the existence of a porous microarchitecture advantageous for drug encapsulation and water uptake. The CL-AX-2 showed clear pH-responsive swelling behavior, with negligible swelling in acidic and higher swelling in alkaline media. This responsiveness illustrates the material's aptitude for site-specific drug administration, especially in gastrointestinal areas like the colon, and indicates the ionization of functional groups within the network. Such potential of CL-AX-2 for regulated and stimuli-triggered drug release is further supported by their reversible swelling–deswelling activity. According to biological analyses, the CL-AX-2 had good hemocompatibility and biocompatibility, with little hemolytic activity. These results validate the CL-AX-2 safety and indicate that the hydrogel system is suitable for biomedical interactions. Furthermore, toxicity evaluations showed that the CL-AX-2 is well-tolerated, supporting its feasibility for other preclinical uses. Overall, the results confirm that CL-AX-2 is an excellent

biomaterial for controlled drug administration, and other therapeutic applications because it combine structural stability, stimuli-responsiveness, and biological safety. This material has the potential to provide a flexible platform for next-generation biopolymer-based medical systems if cross-linking density, drug loading efficiency, and *in vivo* performance are further optimized.

Ethical statement

All animal procedures were performed in accordance with the Guidelines for Care and Use of Laboratory Animals of NIH (National Institutes of Health) and OECD (Organization for Economic Co-operation and Development), and approved by the Institutional Research Ethics Committee of The University of Lahore, Lahore, vide letter No. IREC-2018-76 M, dated May 17, 2018.[44,45]

Author contributions

Syed Nasir Abbas Bukhari: project administration, writing – review & editing, resources. Maryam Fatima: investigation, methodology. Arshad Ali: writing – original draft, formal analysis. Tehreem Fatima: investigation. Muhammad Ajaz Hussain: conceptualization, supervision, writing – review & editing. Haifa Mhaoash Alenzi: formal analysis. Mohamed Abdelwahab Abdelgawad: validation. Mohammad M. Al-Sanea: writing – review & editing. Naveed Ahmad: data curation, methodology.

Conflicts of interest

There are no conflicts to declare.

Data availability

All data generated or analyzed during this study are included in this published article.

Supplementary information (SI) is available. See DOI: https://doi.org/10.1039/d6ra00517a.

Acknowledgements

References

1 A. Abbas, M. A. Raza, X. Ai, Sadia, H. Liao, N. Li, S. Naseer, D. Li, Y. Zhang, L. Chen and W. Zhang, *J. Biomater. Sci., Polym. Ed.*, 2025, **36**, 2490–2512, DOI: 10.1080/09205063.2025.2511992.

2 A. S. Hoffman, Hydrogels for biomedical applications, *Adv. Drug Delivery Rev.*, 2012, **64**, 18–23, DOI: 10.1016/j.addr.2012.09.010.

3 H. Lu, M. Cui, Y. Wang, X. Du, X. Zhou, Y. Fang, X. Gao, Y. Peng, J. Zhu, G. Yang and F. Li, *Nano Res.*, 2025, **18**, 94907012, DOI: 10.26599/NR.2025.94907012.

4 Y. Wang, C. Deng, Y. Ding, S. Huang, S. Chen, H. Huang, S. Yang and F. Xiao, *Colloids Surf., B*, 2025, **254**, 114797, DOI: 10.1016/j.colsurfb.2025.114797.

5 E. Caló and V. V. Khutoryanskiy, *Eur. Polym. J.*, 2015, **65**, 252–267, DOI: 10.1016/j.eurpolymj.2014.11.024.

6 J. Luo, Y. Wang, H. Huang, S. Chen, W. Du, S. Yang and F. Xiao, *Int. J. Biol. Macromol.*, 2025, **333**, 148849, DOI: 10.1016/j.ijbiomac.2025.148849.

7 W. Du, H. Li, J. Luo, Y. Wang, Q. Xi, J. Liu, S. Yang, J. Li and F. Xiao, *Cellulose*, 2024, **31**, 6373–6385, DOI: 10.1007/s10570-024-05972-z.

8 Q. Long, G. Jiang, J. Zhou, D. Zhao and H. Yu, *Research*, 2024, **7**, 0533, DOI: 10.34133/research.0533.

9 J. Liu, J. Chen, S. Liu, T. Li, Y. Chen, L. Chen, R. Cai, X. Liao, T. Zhao and Y. Chen, *Mater. Horiz.*, 2025, **12**, 7473–7485, DOI: 10.1039/D5MH00465A.

10 Y. Zhao, G. Jiang, S. Zeng, L. Sun, H. Yu and D. Zhao, *Adv. Funct. Mater.*, 2025, **36**, e16610, DOI: 10.1002/adfm.202516610.

11 Q. Wang, S. Feng, L. Zhong, Y. Zhou, J. Liu, H. Liu and Q. Zhu, *Int. J. Biol. Macromol.*, 2026, **347**, 150776, DOI: 10.1016/j.ijbiomac.2026.150776.

12 X. Li, X. Kong, Z. Zhang, K. Nan, L. Li, X. Wang and H. Chen, *Int. J. Biol. Macromol.*, 2012, **50**, 1299–1305, DOI: 10.1016/j.ijbiomac.2012.03.008.

13 X. Xue, Y. Hu, Y. Deng and J. Su, *Adv. Funct. Mater.*, 2021, **31**, 2009432, DOI: 10.1002/adfm.202009432.

14 M. H. Fischer, N. Yu, G. R. Gray, J. Ralph, L. Anderson and J. A. Marlett, *Carbohydr. Res.*, 2004, **339**, 2009–2017, DOI: 10.1016/j.carres.2004.05.023.

15 M. Patel and A. Shah, *Int. J. Biol. Macromol.*, 2017, **102**, 1270–1277, DOI: 10.1111/1541-4337.70297.

16 S. Mukherjee, C. A. Pujol, S. Jana, E. B. Damonte, B. Ray and S. Ray, *Carbohydr. Polym.*, 2021, **256**, 117555, DOI: 10.1016/j.carbpol.2020.117555.

17 L. Strkalj, G. E. Yakubov, R. A. Burton and J. M. Compr, *Compr. Rev. Food Sci. Food Saf.*, 2025, **24**, e70297, DOI: 10.1111/1541-4337.70297.

18 N. Fernandez, C. Lopez, R. Diez, J. J. Garcia, M. J. Diez, A. Sahagun and M. Sierra, *Expert Opin. Drug Metab. Toxicol.*, 2012, **8**, 1377–1386, DOI: 10.1517/17425255.2012.716038.

19 A. R. Shah, P. Sharma, T. Longvah, V. S. Gour, S. L. Kothari, Y. R. Shah and S. A. Ganie, *Nut, Today*, 2020, **55**, 313–321, DOI: 10.1097/NT.0000000000000450.

20 A. G. Schioldan, S. Gregersen, S. Hald, A. Bjørnshave, M. Bohl, B. Hartmann, J. J. Holst, H. Stødkilde-Jørgensen and K. Hermansen, Europ, *J. Nutr.*, 2018, **57**, 795–807, DOI: 10.1007/s00394-016-1369-8.

21 B. Singh, V. Sharma, R. Kumar and M. Mohan, *Food Hydrocolloids Health*, 2022, **2**, 100059, DOI: 10.1016/j.fhfh.2022.100059.

22 W. Kaialy, P. Emami, K. Asare-Addo, S. Shojaee and A. Nokhodchi, *Des. Technol.*, 2014, **19**, 269–277, DOI: 10.3109/10837450.2013.775156.

23 J. Irfan, M. A. Hussain, M. T. Haseeb, A. Ali, M. Farid-ul-Haq, T. Tabassum, S. Z. Hussain, I. Hussain and M. Naeem-ul-Hassan, *RSC Adv.*, 2021, **11**, 19755–19767, DOI: 10.1039/D1RA02219A.

24 M. S. Izydorczyk and C. G. Biliaderis, *Carbohydr. Polym.*, 1995, **28**, 33–48, DOI: 10.1016/0144-8617(95)00077-1.

25 M. Waleed, F. Saeed, M. Afzaal, B. Niaz, M. A. Raza, M. Hussain, T. Tufail, A. Rasheed, H. Ateeq and E. Al Jbawi, *Int. J. Food Prop.*, 2022, **25**, 2505–2513, DOI: 10.1080/10942912.2022.2143522.

26 S. Saghir, M. S. Iqbal, M. A. Hussain, A. Koschella and T. Heinze, *Carbohydr. Polym.*, 2008, **74**, 309–317, DOI: 10.1016/j.carbpol.2008.02.019.

27 M. U. A. Khan, S. I. A. Razak, A. Hassan, S. Qureshi and G. M. Stojanović, *Front. Bioeng. Biotechnol.*, 2022, **10**, 865059, DOI: 10.3389/fbioe.2022.865059.

28 M. U. A. Khan, M. A. Raza, S. I. A. Razak, M. R. Abdul Kadir, A. Haider, S. A. Shah, A. H. Mohd Yusof, S. Haider, I. Shakir and S. Aftab, *J. Tissue Eng. Regener. Med.*, 2010, **14**, 1488–1501, DOI: 10.1002/term.3115.

29 J. Irfan, A. Ali, M. A. Hussain, M. T. Haseeb, M. Naeem-ul-Hassan and S. Z. Hussain, *RSC Adv.*, 2024, **14**, 8018–8027, DOI: 10.1039/D4RA00095A.

30 A. Ali, A. Akram, A. B. Siddique, H. M. Amin, L. Zohra, A. Abbas, M. Sher, M. A. Hussain, M. T. Haseeb and M. Imran, *J. Ind. Eng. Chem.*, 2025, **151**, 746–761, DOI: 10.1016/j.jiec.2025.04.046.

31 A. Ali, M. A. Hussain, M. T. Haseeb, S. N. A. Bukhari, T. Tabassum, M. Farid-ul-Haq and F. A. Sheikh, *J. Drug Deliv. Sci. Technol.*, 2022, **69**, 103144, DOI: 10.1016/j.jddst.2022.103144.

32 F. Amjad, A. Ali, M. A. Hussain, M. T. Haseeb, M. Farid-ul-Haq, I. Ajaz, M. Sher and M. Imran, *Mater. Adv.*, 2026, **7**, 1495–1507, DOI: 10.1039/D5MA01018G.

33 V. S. Ghorpade, K. K. Mali, R. J. Dias, S. C. Dhawale, R. R. Digole, J. M. Gandhi, K. A. Bobde and R. K. Mali, *Int. J. Biol. Macromol.*, 2024, **282**, 137127, DOI: 10.1016/j.ijbiomac.2024.137127.

34 M. A. Hussain, A. I. Rana, M. T. Haseeb, G. Muhammad and L. Kiran, *J. Drug Deliv. Sci. Technol.*, 2020, **55**, 101470, DOI: 10.1016/j.jddst.2019.101470.

35 M. W. Abebe, R. A. Ntiamoah and H. Kim, Alginate/chitosan bi-layer hydrogel as a novel tea bag with in-cup decaffeination, *React. Funct. Polym.*, 2022, **170**, 105128, DOI: 10.1016/j.reactfunctpolym.2021.105128.

36 A. Ali, M. A. Hussain, M. T. Haseeb, M. U. Ashraf, M. Farid-ul-Haq, T. Tabassum, G. Muhammad and A. Abbas, *J. Braz. Chem. Soc.*, 2023, **34**, 906–917, DOI: 10.21577/0103-5053.20230001.

37 O. R. Arndt, R. Baggio, A. K. Adam, J. Harting, E. Franceschinis, P. Kleinebudde and J. Pharmaceut, *Sci.*, 2018, **107**, 3143–3152, DOI: 10.1016/j.xphs.2018.09.006.

38 J. G. Wagner, *J. Pharm. Sci.*, 1969, **58**, 1253–1257, DOI: 10.1002/jps.2600581021.

39 R. W. Korsmeyer, R. Gurny, E. Doelker, P. Buri and N. A. Peppas, *Int. J. Pharm.*, 1983, **15**, 25–35, DOI: 10.1016/0378-5173(83)90064-9.

40 P. L. Ritger and N. A. Peppas, *J. Controlled Release*, 1987, **5**, 37–42, DOI: 10.1016/0168-3659(87)90035-6.

41 ISO (International Organization for Standardization), (2002), *Selections of Tests for Interaction with Blood, 10993-4:2002*.

42 American Society for Testing and Materials (ASTM), *Standard Practice for Assessment of Hemolytic Properties of Materials*, ASTM International, West Conshohocken (PA), 2008.

43 A. Ali, M. A. Hussain, M. T. Haseeb, S. N. A. Bukhari, G. Muhammad, F. A. Sheikh and M. Farid-ul-Haq, Curr, *Drug Deliv.*, 2023, **20**, 292–305, DOI: 10.2174/1567201819666220509200019.

44 OECD (Organization for Economic Co-operation and Development) Guidelines for Testing of Chemicals. Acute Oral Toxicity-Fixed Dose ProcedureNo. **420** (2001), https://ntp.niehs.nih.gov/iccvam/suppdocs/feddocs/oecd/oecd_gl420.pdf.

45 OECD (Organization for Economic Co-operation and Development) Guidelines for Testing of Chemicals. Acute Dermal Toxicity: Fixed Dose ProcedureNo. **402** (2017), doi: DOI: 10.1787/9789264070585-en.

46 J. H. Draize, *J. Pharmacol. Exp. Ther.*, 1944, **82**, 377–390, https://jpet.aspetjournals.org/content/82/3/377.

47 Z. M. Saiyad, K. Sengupta, A. V. Krishnaraju, G. Trimurtula, F. C. Lau and J. P. Lugo, *Food Chem. Toxicol.*, 2015, **78**, 122–129, DOI: 10.1016/j.fct.2015.02.010.

48 A. Ali, M. A. Hussain, A. Abbas, M. T. Haseeb, I. Azhar, G. Muhammad, S. Z. Hussain, I. Hussain and N. F. Alotaibi, *J. Mol. Liq.*, 2023, **376**, 121438, DOI: 10.1016/j.molliq.2023.121438.

49 Z. Wang, Y. Tian and A. V. Dobrynin, *Macromolecules*, 2023, **56**, 6543–6551, DOI: 10.1021/acs.macromol.3c01034.

50 R. De Piano, D. Caccavo, A. A. Barba and G. Lamberti, *Gels*, 2024, **10**, 813, DOI: 10.3390/gels10120813.

51 B. A. Lodhi, M. A. Hussain, M. Sher, M. T. Haseeb, M. U. Ashraf, S. Z. Hussain, I. Hussain and S. N. A. Bukhari, *Adv. Polym. Technol.*, 2019, **2019**, 9583516, DOI: 10.1155/2019/9583516.